Oncology Research, Vol. 28, pp. 331–344
Printed in the USA.

0965-0407/20 $90.00 + .00
DOI: https://doi.org/10.3727/096504020X15825405463920
E-ISSN 1555-3906
www.cognizantcommunication.com

A Novel BCL-2 Inhibitor APG-2575 Exerts Synthetic Lethality With BTK or MDM2-p53 Inhibitor in Diffuse Large B-Cell Lymphoma

Qiuyun Luo,*†[1] Wentao Pan,*†‡[1] Suna Zhou,*†[1] Guangfeng Wang,‡ Hanjie Yi,*§ Lin Zhang,*¶ Xianglei Yan,*† Luping Yuan,*† Zhenyi Liu,# Jing Wang,** Haibo Chen,# MiaoZhen Qiu,*†† DaJun Yang,*†‡ and Jian Sun*‡‡

*State Key Laboratory of Oncology in South China, Collaborative Innovation Center for Cancer Medicine, Guangzhou, P.R. China
†Department of Experimental Research, Sun Yat-Sen University Cancer Center, Guangzhou, P.R. China
‡Suzhou Ascentage Pharma Inc., Jiangsu, P.R. China
§The Second Affiliated Hospital of Nanchang University, Nanchang, P.R. China
¶University Department of Clinical Laboratory, Sun Yat-Sen University Cancer Center, Guangzhou, P.R. China
#Peking University Shenzhen Hospital, Shenzhen, P.R. China
**Guangzhou Red Cross Hospital, Guangzhou, P.R. China
††Department of Medical Oncology, Sun Yat-Sen University Cancer Center, Guangzhou, P.R. China
‡‡Department of Clinical Research, Sun Yat-Sen University Cancer Center, Guangzhou, P.R. China

Despite therapeutic advances, the effective treatment for relapsed or refractory diffuse large B-cell lymphoma (DLBCL) remains a major clinical challenge. Evasion of apoptosis through upregulating antiapoptotic B-cell lymphoma-2 (BCL-2) family members and p53 inactivation, and abnormal activation of B-cell receptor signaling pathway are two important pathogenic factors for DLBCL. In this study, our aim is to explore a rational combination of BCL-2 inhibitor plus Bruton's tyrosine kinase (BTK) blockade or p53 activation for treating DLBCL with the above characteristics. We demonstrated that a novel BCL-2 selective inhibitor APG-2575 effectively suppressed DLBCL with BCL-2 high expression via activating the mitochondrial apoptosis pathway. BTK inhibitor ibrutinib combined with BCL-2 inhibitors showed synergistic antitumor effect in DLBCL with mean expression of BCL-2 and myeloid cell leukemia-1 (MCL-1) through upregulating the expression level of BIM and modulating MCL-1 and p-Akt expression. For p53 wild-type DLBCL with high expression of BCL-2, APG-2575 showed strong synergic effect with mouse double minute 2 (MDM2)–p53 inhibitor APG-115 that can achieve potent antitumor effect and markedly prolong survival in animal models. Collectively, our data provide an effective and precise therapeutic strategy through rational combination of BCL-2 and BTK or MDM2–p53 inhibitors for DLBCL, which deserves further clinical investigation.

Key words: B-cell lymphoma-2 (BCL-2); Apoptosis; Small molecule inhibitor; Diffuse large B-cell lymphoma (DLBCL); Combination therapy

INTRODUCTION

Diffuse large B-cell lymphoma (DLBCL) is the most common subtype of non-Hodgkin lymphoma (NHL), comprising about 30% of the NHL throughout the world[1,2]. Even with therapy development, some patients with relapsed or refractory DLBCL remain incurable[3,4]. Therefore, there is an urgent need to develop new treatment for these patients.

B-cell lymphoma-2 (BCL-2) overexpression, which inhibits tumor cell apoptosis, is presented in about 25% of DLBCL and is associated with poor prognosis[5,6]. Previous studies suggested that BCL-2 may be a potential target for the treatment of DLBCL[7,8]. A series of BH3 mimetic small molecules that bind to antiapoptotic proteins such as BCL-2 and BCL-XL have been developed for tumor therapy[9–12] and have shown promising results in phase I and II clinical trials in several types of cancer[13–15].

[1]These authors provided equal contribution to this work.
Address correspondence to Professor Jian Sun, Department of Clinical Research, Sun Yat-Sen University Cancer Center, 651 Dongfeng Road East, Guangzhou 510060, China. Tel: +86 20 8734 3827; Fax: +86 20 8734 3827; E-mail: sunjian@sysucc.org.cn *or* Professor Dajun Yang, Department of Experimental Research, Sun Yat-Sen University Cancer Center, 651 Dongfeng Road East, Guangzhou 510060, China. Tel: +86 20 8734 2285; Fax: +86 20 8734 2285; E-mail: yangdj@sysucc.org.cn

However, several hematology-derived cell lines remain resistant to BCL-2 inhibitors, particularly the very heterogeneous DLBCL tumor cells. Aberrant activation of B-cell receptor (BCR) signaling pathway mediated by Bruton's tyrosine kinase (BTK) is also another important pathogenic factor in partial B-cell NHLs including DLCBL[16–18]. BTK inhibitors such as ibrutinib have been reported to show great potential in the treatment of B-cell NHLs[19,20], but have limited efficacy as single agents[16,21]. It has been shown that BCL-2 inhibition can enhance the antitumor effect of ibrutinib, which is one of the approaches to overcome the limited efficacy of ibrutinib monotherapy[22].

TP53 is an important tumor suppressor gene that is less mutated in DLBCL[23]. However, wild-type p53 functions are frequently inhibited by mouse double minute 2 (MDM2), which is another important pathway for cancer cells to escape apoptosis[24,25]. It has been suggested that high expression of myeloid cell leukemia-1 (MCL-1) may contribute to intrinsic and acquired resistance to BCL-2 inhibitors[26,27], while p53 activation can modulate MCL-1 phosphorylation and promote its degradation[28]. Therefore, the combination of BCL-2 inhibitor and MDM2–p53 inhibitor will provide a rational and effective treatment and achieve better antitumor efficacy.

The aim of this study was to investigate the antitumor effect of a novel selective BCL-2 inhibitor APG-2575 in combination with the BTK inhibitor ibrutinib or MDM2–p53 inhibitor in a rational combination in DLBCL based on the molecular biological properties of DLBCL, and further to study its mechanism of action. Thus, we hope that these preclinical data can provide a more solid theoretical basis for improving the clinical treatment of DLBCL.

MATERIAL AND METHODS

Chemicals

A novel BCL-2 selective inhibitor APG-2575 and MDM2–p53 inhibitor APG-115 were provided by Ascentage Pharma Group Inc. (Taizhou, China). BCL-2 selective inhibitor ABT-199 and BTK inhibitor ibrutinib were purchased from Selleck Chemicals (Houston, TX, USA). The binding affinities of APG-2575 and reference compounds ABT-199 and ABT-263 to BCL-2, BCL-XL, and MCL-1 are shown in Table 1. For in vitro assay, all compounds were dissolved in dimethyl sulfoxide (DMSO; Sigma-Aldrich, St. Louis, MO, USA) at a stock concentration of 40 mM, stored at −20°C. The final concentration of DMSO to dilute compound in culture media did not exceed 0.1%. For in vivo study, APG-2575 was formulated in 60% phosal 50 propylene glycol, 30% polyethylene glycol 400 (PEG 400), and 10% ethanol; ibrutinib was in 5% DMSO, 30% PEG 300, 5% Tween 80, and ddH_2O; APG-115 was formulated in 5% PEG 400 and 95% 0.2% HPMC E5.

Cell Culture

The cell lines OCI-LY1, OCI-LY3, OCI-LY19, and SU-DHL4 were purchased from Leibniz-Institut DSMZ-German Collection of Microorganisms and Cell Cultures (DSMZ, Braunschweig, Germany) and the American Type Culture Collection (ATCC; Manassas, VA, USA) provided by Cobioer Biological Technology Co. Ltd. (Nanjing, China). The SU-DHL2 and OCI-LY8 cell lines were provided by Professor Wenqi Jiang in Sun Yat-sen University Cancer Center. All these cell lines were identified by genomic short tandem repeat (STR) profile detection, which was provided by Cobioer Biological Technology Co. Ltd. (Nanjing, China). All cells were cultured at 37°C, in a humidified atmosphere containing 5% CO_2. OCI-LY8, SU-DHL2, and SU-DHL4 cells were cultured in RPMI-1640 medium containing 10% fetal bovine serum, while OCI-LY3 cells were cultured in RPMI-1640 medium containing 20% fetal bovine serum. OCI-LY1 cells were maintained in IMDM medium supplemented with 20% fetal bovine serum, while OCI-LY19 cells were maintained in α-MEM medium supplemented with 10% FBS. All culture media contained 100 IU/ml penicillin and 100 mg/ml streptomycin. All experiments were performed in the logarithmic growth phase of the cells.

Cell Viability Assay and IC_{50} Determination

Cell viability was determined by using the Cell Counting Kit-8 (CCK-8; Dojindo, Japan) according to the manufacturer's instructions. Briefly, cells were seeded at 20,000 to 50,000 cells/well in a 96-well plate in the presence of single drugs or drug combinations for 48 h. After 48 h, CCK-8 reagent (10 μl/well) was added and incubated at 37°C for 1–2 h, and absorbance readings were

Table 1. Binding Affinities of APG-2575 and Reference Compounds to BCL-2, BCL-XL, and MCL-1

Target	Drugs	BCL-2 (nM) K_i	BCL-XL (nM) K_i	BCL-W (nM) K_i	MCL-1 (nM) K_i
BCL-2/BCL-XL	ABT-263*	1	<0.5	1	No binding affinity
BCL-2	ABT-199*	<0.1	<0.5	No	No binding affinity
BCL-2	APG-2575	<0.1	<0.5	No	No binding affinity

*Data from Selleck (https://www.selleck.cn/).

taken at 450 nm. The IC_{50} value was calculated by using GraphPad Prism version 6.0.0 for Windows (GraphPad Software, San Diego, CA, USA). Combination index (CI) is a marker to reflect the drug interaction, which was evaluated by using the CalcuSyn software (BIOSOFT, Ferguson, MO, USA). The criteria for the CI value are as follows: $0.8 \leq CI < 1$ for low synergy, $0.6 \leq CI < 0.8$ for moderate synergy, $0.4 \leq CI < 0.6$ for high synergy, and $0.2 \leq CI < 0.4$ for strong synergy effect.

Cell Apoptosis Assays and Mitochondrial Membrane Potentials Detection

Cell apoptosis was determined with an Annexin-V–propidium iodide (PI) apoptosis detection kit (KGA108; KeyGen Biotech, Nanjing, China) by flow cytometry (Beckman Coulter, Fullerton, CA, USA). Cells were harvested and suspended in 500 µl of binding buffer containing 2.5 µl of annexin V fluorescein isothiocyanate (FITC) and 5 µl of PI. Experiments were analyzed after incubating out of light in the staining solution for 10 min.

Flow cytometry was used for the detection of mitochondrial membrane potential change. Briefly, after APG-2575 treatment, the cells were incubated with 5 mg/L JC-1 (Beyotime Biotech, Jiangsu, China) for 20 min at 37°C, and then cells were washed twice with JC-1 staining buffer (1×). Using some JC-1 staining buffer (1×), resuspended cells were analyzed by flow cytometry.

Detection of Caspase 3 Activity

The activity of caspase 3 was determined using the caspase 3 activity kit (Beyotime Institute of Biotechnology, Haimen, China). After treatment of APG-2575, cell lysates were prepared by incubating 2×10^6 cells/ml in extraction buffer (25 mM Tris HCl, pH 7.5, 20 mM $MgCl_2$, and 150 mM NaCl, 1% Triton X-100, 25 µg/ml leupeptin, and 25 µg/ml aprotinin) for 30 min on ice. Lysates were centrifuged at 12,000 × *g* for 15 min, the supernatants were collected, and protein concentration was determined by Bradford Protein Assay Kit (Beyotime Institute of Biotechnology, Haimen, China). Cellular extracts (30 µg) were then incubated in a 96-well plate with 20 ng of Ac-DEVD-pNA for 2 h at 37°C. Caspase 3 activity was measured by cleavage of the Ac-DEVD-pNA substrate to pNA, the absorbance of which was measured at 405 nm. Relative caspase activity was calculated as a ratio of emission of treated cells to untreated cells.

Western Blot Analysis

Western blot analysis was performed by standard methods as previously described[29]. The antibodies against BCL-2, BCL-XL, MCL-1, BAX, BAK, cleaved caspase 3, cytochrome c, glyceraldehyde 3-phosphate dehydrogenase (GAPDH), Akt, p-Akt, and β-tubulin were purchased from Cell Signaling Technology. The antibodies against PARP, BIM, p53, MDM2, and PUMA were purchased from Santa Cruz Biotechnology (Santa Cruz, CA, USA). The antibody against BTK was purchased from ImmunoWay Biotechnology (JiangSu, China). The secondary anti-mouse and anti-rabbit antibodies were purchased from Santa Cruz Biotechnology. Antigen–antibody complexes were detected using Bio-Rad Clarity western ECL substrate, and protein level was quantified by ImageJ (Bio-Rad Laboratory, Hercules, CA, USA).

Mitochondrial Cytochrome c Release Assay

Cells were pretreated with 20 nmol/l of APG-2575 for 0, 0.5, 1, 3, and 6 h. Cytoplasmic fractionation was isolated using the Cytosol/Mitochondria Fractionation kit (#QIA88; Merck Millipore, Darmstadt, Germany). Cytosolic fractions were isolated from OCI-LY8 cells following the manufacturer's instruction. The amount of cytochrome c in cytosol and mitochondria fraction was determined by Western blot analysis as described above.

In Vivo Treatment of Xenografts With APG-2575

All animal studies were performed with the approval from the Institutional Animal Care and Use Committee (IACUC) of Sun Yat-sen University Cancer Center (IACUC Approval No. 17040M). To develop OCI-LY8, OCI-LY1, and OCI-LY19 xenograft, 4- to 6-week-old female nonobese diabetic severe combined immunodeficiency (NOD/SCID) mice (Beijing Vital River Laboratory Technology Co. Ltd, Beijing, China) were implanted subcutaneously in the right side of the axillary with 1×10^7 tumor cells suspended in 100-µl volume of PBS containing Matrigel (Corning, Corning, NY, USA) at 1:1 ratio. OCI-LY8 models were used for APG-2575 single-drug efficacy studies; when mean tumor volume reached approximately 100~200 mm^3, mice were randomized into four groups (six mice per group) with approximately equivalent tumor volume. The mice were treated with vehicle or APG-2575 (25 mg/kg, 50 mg/kg, and 100 mg/kg body weight) daily by oral gavage for 10 days. In OCI-LY1 models applied to study, the combination efficacy of APG-2575 and ibrutinib, mice were randomly divided into four groups (five mice per group) with approximately equivalent tumor volume, and the treatment was started on day 1. Mice were treated with 15 mg/kg ibrutinib or vehicle at day 1 by intraperitoneal injection once a day for 13 consecutive days, while 100 mg/kg APG-2575 administered via oral gavage started at day 8 of six consecutive days. OCI-LY19 models were used to study the combination antitumor effect of APG-2575 and APG-115; mice were randomized into four groups (five mice per group) with approximately equivalent tumor volume. Vehicle, 50 mg/kg APG-2575, 50 mg/kg APG-115, and combination are administered orally once every day for 6 days. Tumor

sizes were measured by caliper equipment, and animal body weights were recorded two to three times per week. Tumor volume (mm^3) = 1/2 × (length × $width^2$).

Immunohistochemical Analyses

Tumor tissues from the NOD/SCID mice were immunohistochemically stained for Ki-67 using previously reported protocols[30]. TUNEL staining was performed with an in situ cell death detection kit (Roche Diagnostics Corp., Mannheim, Germany) according to the manufacturer's instructions. The representative images were taken using an Olympus FV1000 microscope (Olympus, Tokyo, Japan).

Statistical Analysis

Statistical analyses were performed in the GraphPad Prism version 6.0.0 for Windows (GraphPad Software). Unless indicated otherwise, results are presented as mean ± standard deviation (SD) of three independent experiments. Correlation was analyzed by nonparametric Spearman correlation. Differences between two groups were analyzed using unpaired sample *t*-test. Comparison among more than two groups was analyzed by one-way analysis of variance (ANOVA) and two-way ANOVA. CI was calculated using CalcuSyn software (BIOSOFT). The Kaplan–Meier method was used to plot survival curves, and log-rank was used to compare survival differences. A value of $p < 0.05$ was considered statistically significant.

RESULTS

High BCL-2 Expression Predicts Sensitivity to BCL-2 Inhibitor

First, we found that the BCL-2 gene expression was higher in DLBCL tumor tissue than the normal tissue

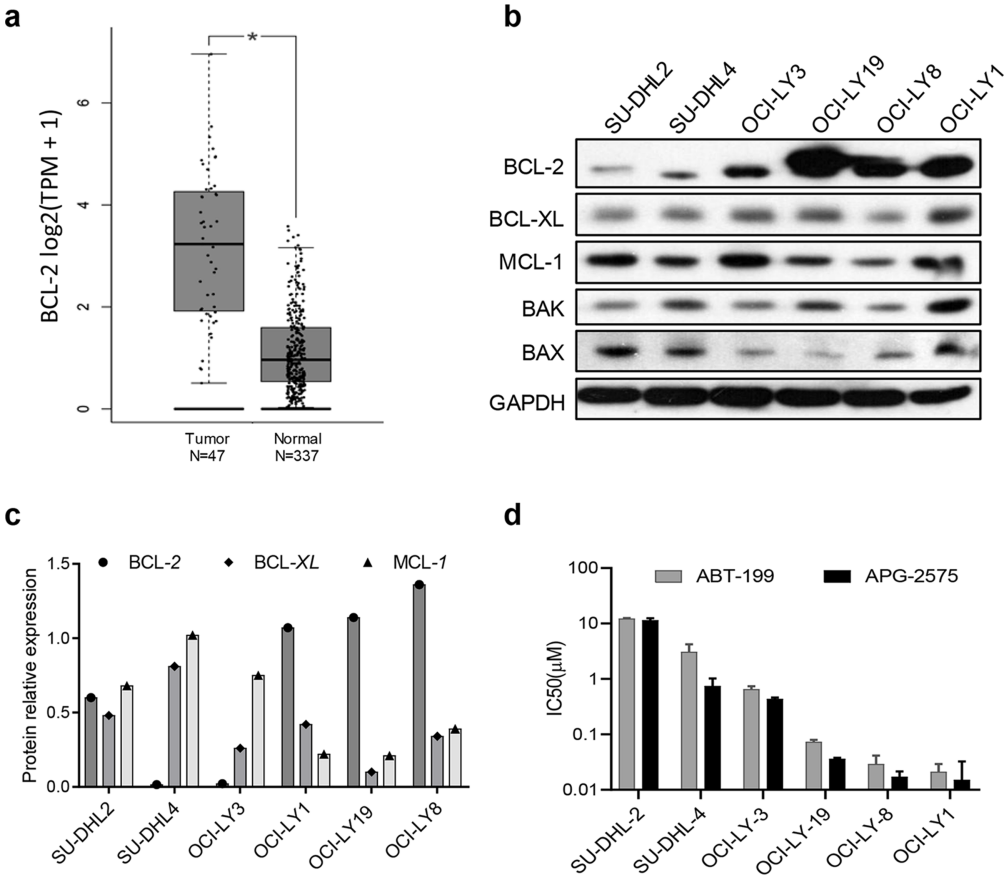

Figure 1. High B-cell lymphoma-2 (BCL-2) expression predicts sensitivity to APG-2575 and APG-1252 in diffuse large B-cell lymphoma (DLBCL). (a) BCL-2 gene expression in DLBCL tissue and normal tissue; data obtained from the GEPIA (Gene Expression Profiling Interactive Analysis) database (http://gepia.cancer-pku.cn/). Statistical significance was determined by unpaired *t*-test. *$p < 0.05$. (b) BCL-2, BCL-XL, MCL-1, BAK, and BAX protein expression were measured by Western blot in DLBCL cell lines with glyceraldehyde 3-phosphate dehydrogenase (GAPDH) as the loading control. (c) The relative protein expression of BCL-2, BCL-XL, and MCL-1 were normalized against GAPDH. (d) Cell viability of DLBCL cell lines treated with APG-2575 and ABT-199 for 48 h, compared to cells treated with dimethyl sulfoxide (DMSO) (100%). The results represent the average and standard deviation (SD) for at least three independent experiments.

Table 2. Cell Killing Activity of APG-2575 and ABT-199 Against Diffuse Large B-Cell Lymphoma Cell Lines

Subtype	Cell Line	APG-2575 IC_{50} (μM) [Mean (SD)]	ABT-199 IC_{50} (μM) [Mean (SD)]
ABC	SU-DHL-2	10.343 (1.719)	12.147 (0.379)
GCB	SU-DHL-4	1.110 (0.537)	3.047 (1.171)
ABC	OCI-LY-3	0.383 (0.059)	0.650 (0.090)
GCB	OCI-LY-19	0.041 (0.006)	0.073 (0.007)
GCB	OCI-LY-8	0.017 (0.006)	0.029 (0.012)
GCB	OCI-LY-1	0.014 (0.002)	0.021 (0.008)

by analyzing the data in the GEPIA (Gene Expression Profiling Interactive Analysis) database (http://gepia.cancer-pku.cn/) (Fig. 1a). We then determined the basic protein expression levels of BCL-2 family members in a panel of six DLBCL cell lines by Western blot analysis. The relative protein expressions of BCL-2, BCL-XL, and MCL-1 were normalized to GAPDH. We found that OCI-LY19, OCI-LY8, and OCI-LY1 had high BCL-2 protein expression, whereas SU-DHL2 and SU-DHL4 had low BCL-2 expression and high MCL-1 expression (Fig. 1b and c). We further verified that DLBCL cells (OCI-LY19, OCI-LY8, and OCI-LY1) with higher BCL-2 expression were more sensitive to the BCL-2 selective inhibitor APG-2575 by CCK-8 assay; the IC_{50} values ranged from 10 to 50 nM (Fig. 1d, Table 2). However, OCI-LY3 and SU-DHL4 cells showed modest response to APG-2575. The inhibitory effect of APG-2575 on BCL-2 high expression cell lines was the same or even better than that of ABT-199. Taken together, DLBCL cell lines with high expression of BCL-2 are sensitive to APG-2.

APG-2575 Induces DLBCL Cell Apoptosis via Activating the Mitochondrial Apoptotic Pathway

After treating with increasing concentrations of APG-2575 for 24 h, we found the apoptosis rate significantly increased in OCI-LY8 and OCI-LY19 cells in a dose-dependent manner (Fig. 2a). APG-2575 induced rapid apoptosis within 4 h in OCI-LY8 and OCI-LY19 cells with high expression of BCL-2 in a time-dependent manner (Fig. 2b). Furthermore, Western blot analysis suggested APG-2575 induced a dose-dependent increase in cleaved PARP and cleaved caspase 3 in OCI-LY8 and OCI-LY19 cells, the well-known characteristic of apoptosis (Fig. 2c).

To determine whether the antitumor effect induced by APG-2575 was associated with the mitochondrial apoptotic pathway, we first measured the mitochondrial membrane potential, which can be measured by flow cytometry using JC-1 staining because mitochondrial membrane potential is affected before membrane evagination occurs in apoptotic cells. The mitochondrial outer membrane permeabilization (MOMP) was significantly decreased by APG-2575 treatment both in OCI-LY8 and OCI-LY19 (Fig. 2d). Next, we assessed the activity of key apoptosis regulator caspase 3 in OCI-LY8 and OCI-LY19 cells. Activity of caspase 3 was significantly increased after APG-2575 treatment (Fig. 2e). Significant activation of caspase 3 and PARP indicated loss of mitochondrial membrane potential. Furthermore, we observed that cytochrome c was released from the mitochondria into the cytoplasm after APG-2575 treatment (Fig. 2f and g), which induced irreversible apoptosis. In summary, APG-2575 leads to cell death via activating the mitochondrial apoptotic pathway in BCL-2-overexpressing DLBCL cells.

APG-2575 Alone Effectively Suppresses Tumor Growth in BCL-2-Overexpressing DLBCL Xenograft Models

We next tested the antitumor efficacy of APG-2575 as monotherapy in vivo. We established a human xenograft DLBCL animal model using the OCI-LY8 cell line with high expression of BCL-2 and low expression of BCL-XL and MCL-1 protein level. Daily oral administration of APG-2575 inhibited OCI-LY8 subcutaneous xenograft tumor growth in a dose-dependent manner. Daily dose of 50 and 100 mg/kg APG-2575 for 10 days resulted in 35.8% and 63.3% tumor inhibition, respectively, compared with the vehicle control group with a mean tumor volume of $2025.3 \pm 195.9\ mm^3$ (Fig. 3a). The measurement of tumor weight at the end of the experiment was also consistent with the above results (Fig. 3b and c). APG-2575 was well tolerated without significant weight loss or other obvious toxicity signs in NOD-SCID mice (Fig. 3d). In situ TUNEL staining further demonstrated that APG-2575 also promoted apoptosis of tumor cells in vivo. TUNEL-positive cells showed typical apoptotic morphology, such as condensation and nuclear fragmentation. Compared to the control group, the number of TUNEL-positive cells was significantly increased in the treatment group, which was consistent with the in vitro results (Fig. 3e and f). In addition, Western blot analysis revealed that APG-2575 led to a dose-dependent increase in cleaved PARP and cleaved caspase 3 in vivo (Fig. 3g).

BCL-2 Inhibition Can Effectively Enhance the Inhibitory Effect of BTK Inhibitor

BTK is a potential therapeutic target for DLBCL. The data generated from the GEPIA database also showed higher expression of BTK genes in DLBCL tissues than in normal tissues (Fig. 4a). Even though the BTK inhibitor ibrutinib has been approved for NHL treatment, its clinical efficacy remains limited. We examined the basic protein expression of BTK in six DLBCL cell lines by Western blot. We found that SU-DHL4 and OCI-LY8 cells had high expression of BTK, while OCI-LY1 and SU-DHL4 cells had slight BTK expression (Fig. 4b). We next tested the IC_{50} of ibrutinib against DLBCL cell lines by CCK-8

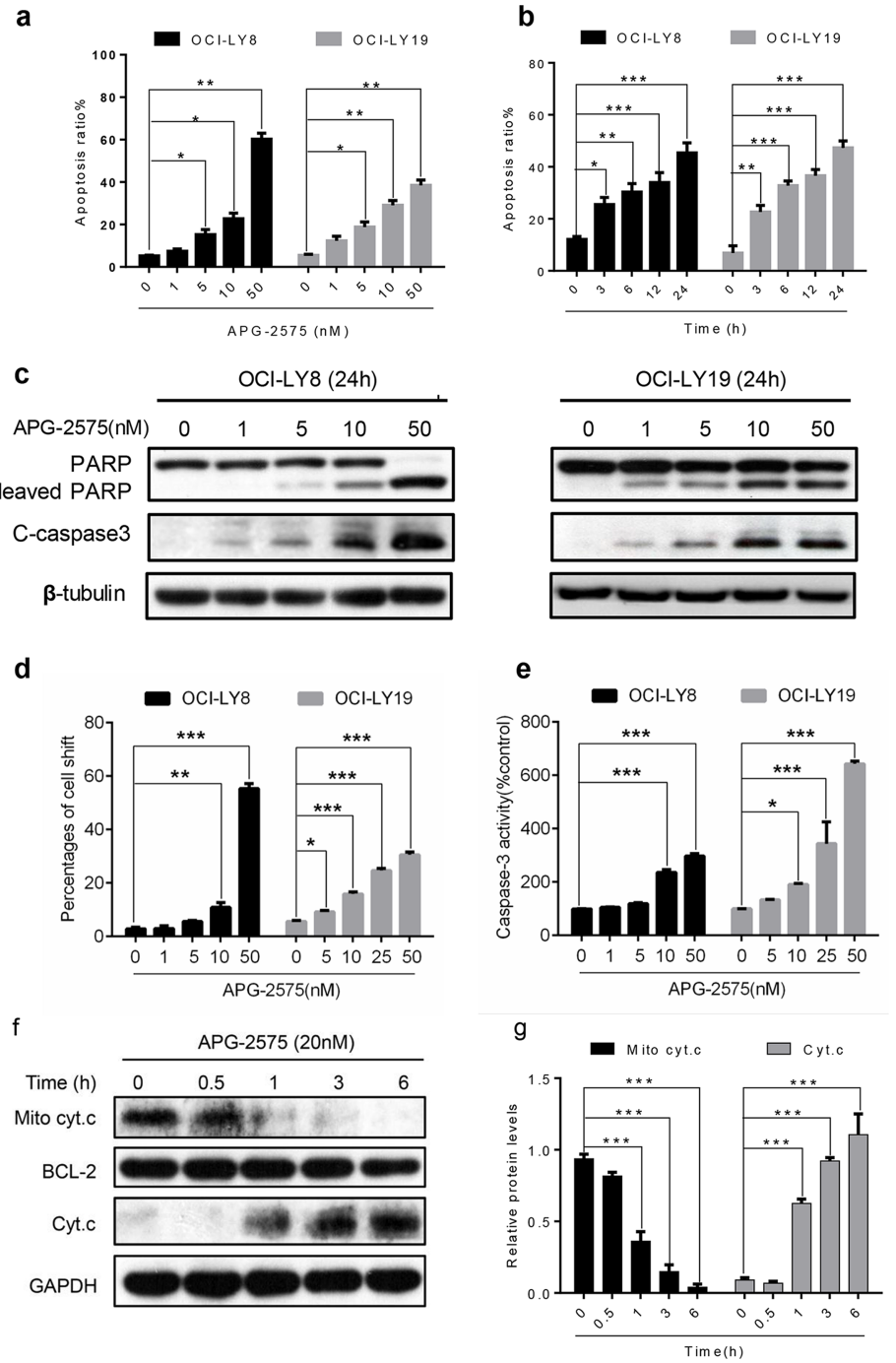

Figure 2. APG-2575 induces apoptosis associated with mitochondria-dependent pathway. (a) OCI-LY8 and OCI-LY19 cells were treated with indicated concentrations of APG-2575 for 24 h and then detected apoptosis by annexin V/propidium iodide (PI) staining and analyzed using flow cytometry. (b) APG-2575 induced a time-dependent apoptosis in OCI-LY8 and OCI-LY19 cells determined by flow cytometry at 25 nM of APG-2575. (c) Western blot analysis to evaluate the protein expression of PARP/cleaved PARP and cleaved caspase 3 change in OCI-LY8 and OCI-LY19 cells treated with indicated concentrations of APG-2575 for 24 h. β-Tubulin was the loading control. (d) Mitochondrial membrane potential detected by JC-1 staining of OCI-LY8 and OCI-LY19 cells treated with indicated concentrations of APG-2575 for 24 h and quantification of the percentages of cells shift. (e) Caspase 3 activity was measured 24 h after adding APG-2575 and was plotted relative to the DMSO control. (f) Cytochrome c (Cyt. c) abundance in mitochondrial and cytosolic fractions of OCI-LY8 were determined by Western blot after 6 h of treatment with increasing concentrations of APG-2575. BCL-2 and GAPDH serve as protein loading controls for the mitochondria and cytosol, respectively. (g) Quantification analysis of Cyt. C relative expression in (f). The data are presented as the mean ± SD of triplicate experiments. Statistical significance was determined by one-way analysis of variance (ANOVA). *$p < 0.05$, **$p < 0.01$, ***$p < 0.001$.

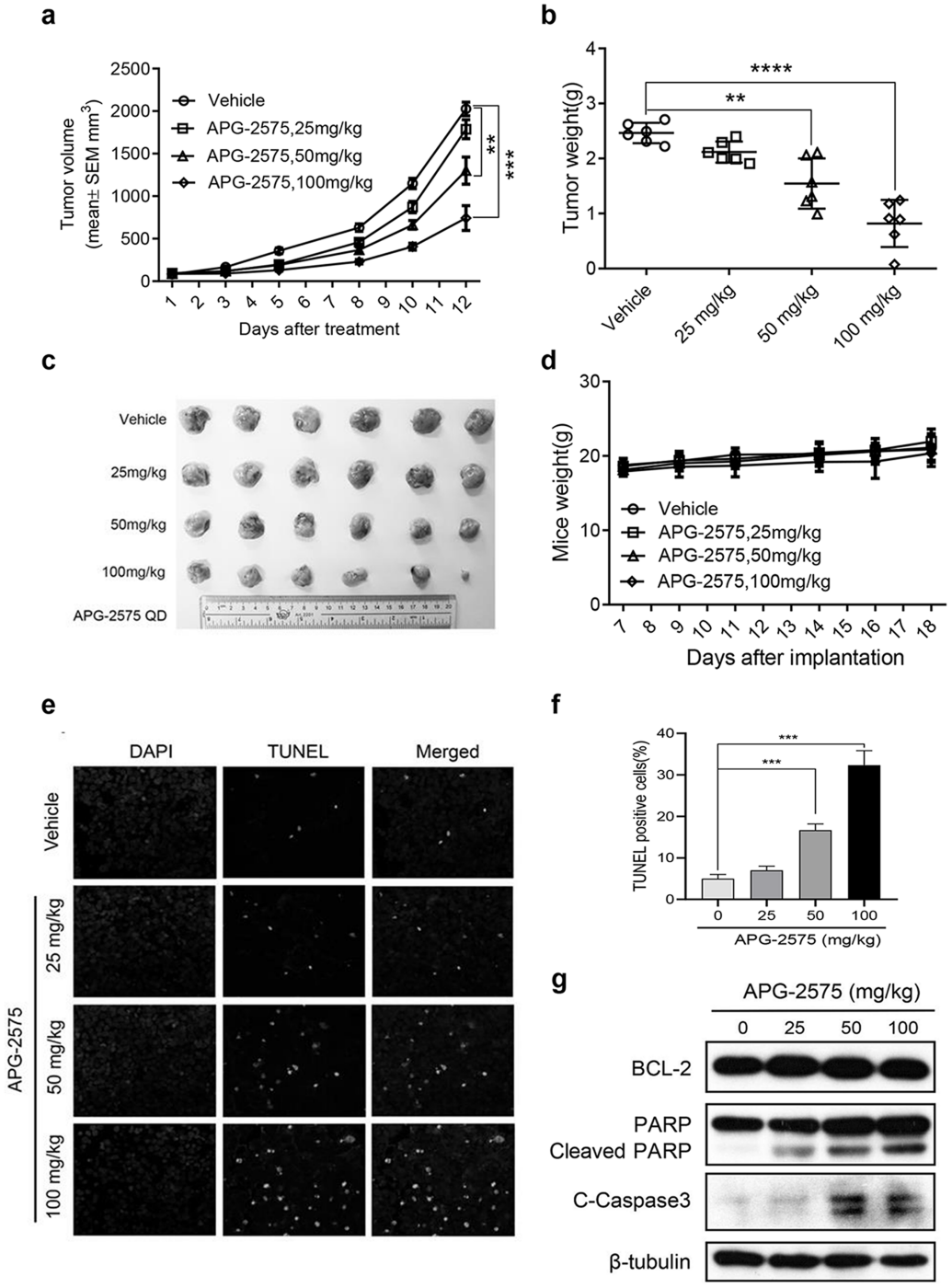

Figure 3. APG-2575 exhibits antitumor activity in DLBCL xenograft models with BCL-2 overexpression. (a) Tumor volumes of OCI-LY8 xenograft models treated with vehicle or APG-2575 (25, 50, and 100 mg/kg). Data are shown as mean ± standard error of the mean (SEM) of six mice in each group. Statistical significance was determined by two-way ANOVA. $^{**}p < 0.01$, $^{***}p < 0.001$. (b) Tumor weight of the four separate groups was recorded at the end of experiment. Data are shown as mean ± SD of six mice in each group. Statistical significance was determined by one-way ANOVA. $^{**}p < 0.01$, $^{***}p < 0.001$. (c) Photographs of harvested tumors of OCI-LY8 tumor-bearing mice. (d) Mice weight of four separate groups was recorded. Data are shown as mean ± SD of six mice in each group. (e) Representative photomicrographs of TUNEL-positive cells and DAPI in xenograft tumors from four separate groups of mice. All images were collected at the same magnification. (f) The mean percentage of TUNEL-positive cells for four groups treated with vehicle, APG-2575 (20 mg/kg), APG-2575 (50 mg/kg), and APG-2575 (100 mg/kg) from three microscopic fields. The data are plotted as mean ± SD. $^{***}p < 0.001$. (g) Western blot analysis of BCL-2, PARP/cleaved PARP, and cleaved caspase 3 protein expression in OCI-LY8 xenograft tumors.

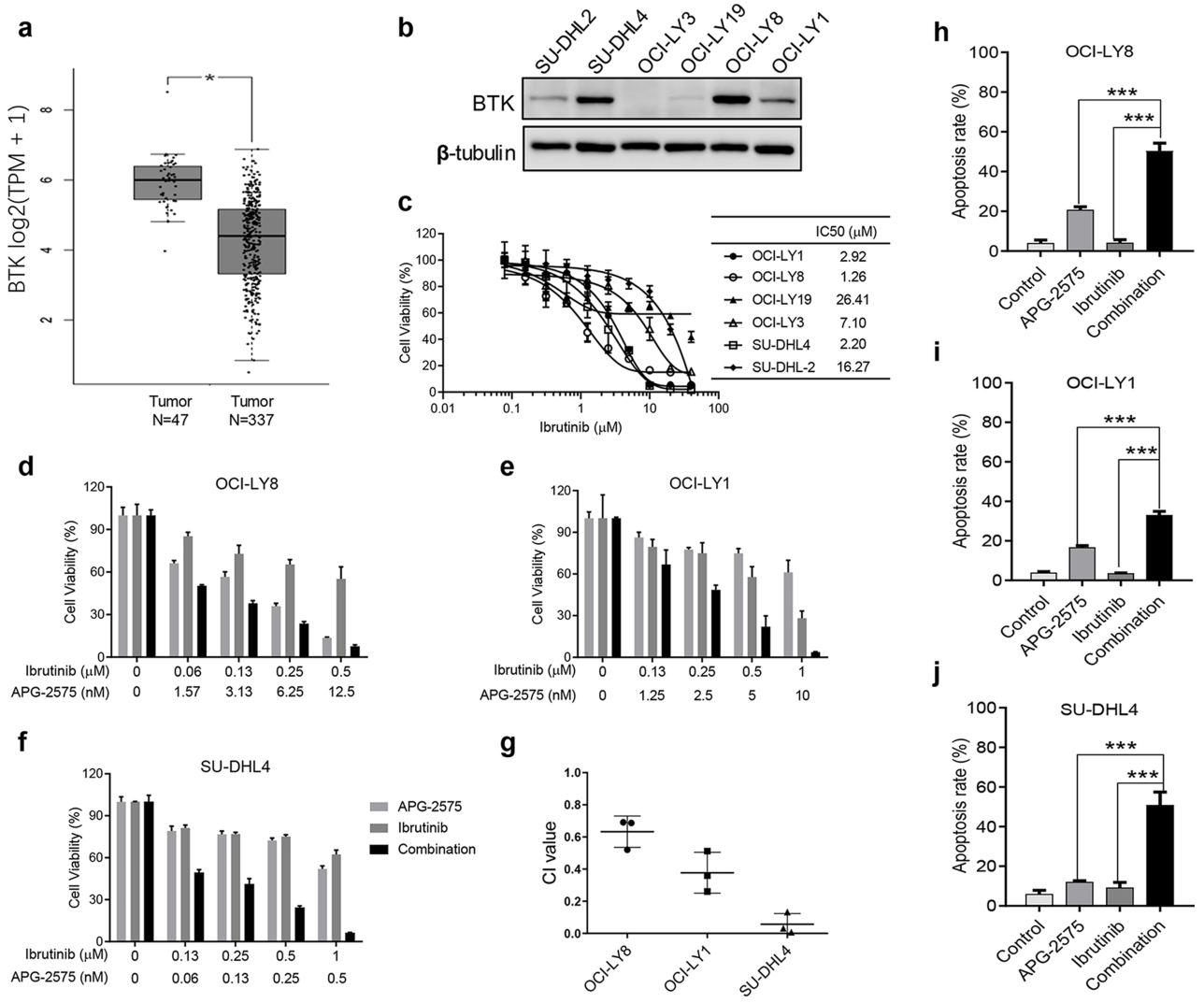

Figure 4. BCL-2 inhibition combined with BTK blockade show synergistic antitumor effect. (a) BTK gene expression in DLBCL tissue and normal tissue; data obtained from the GEPIA (Gene Expression Profiling Interactive Analysis) database (http://gepia.cancer-pku.cn/). Statistical significance was determined by unpaired *t*-test. $*p < 0.05$. (b) BTK protein expression were measured by Western blot in DLBCL cell lines with β-tubulin as the loading control. (c) Cell viability detection for IC_{50} of DLBCL cell lines treated with BTK inhibitor ibrutinib for 48 h, relative to cells treated with DMSO (100%). The results represent the average and SD for at least three independent experiments. (d) Cell viability of OCI-LY8 cells after treatment with ibrutinib, APG-2575, or the combination at indicated concentrations for 48 h. (e) Cell viability of OCI-LY1 cells after treatment with ibrutinib, APG-2575, or the combination at indicated concentrations for 48 h. (f) Cell viability of SU-DHL4 cells after treatment with ibrutinib, APG-2575, or the combination at indicated concentrations for 48 h. (g) Combination index (CI) value of ibrutinib and APG-2575 combination in OCI-LY8, OCI-LY19, and SU-DHL4 cells. (h) OCI-LY8 cells were treated with DMSO, APG-2575 (10 nM), ibrutinib (1 μM), or combination of both agents for 24 h, and drug effect on apoptosis was determined by annexin V/PI staining and analyzed using flow cytometry. (i) OCI-LY1 cells were treated with DMSO, APG-2575 (10 nM), ibrutinib (1 μM), or combination of both agents for 24 h, and drug effect on apoptosis was determined by annexin V/PI staining and analyzed using flow cytometry. (j) SU-DHL4 cells were treated with DMSO, APG-2575 (50 nM), ibrutinib (1 μM), or the combination of both agents for 24 h, and drug effect on apoptosis was determined by annexin V/PI staining and analyzed using flow cytometry. The data are presented as the mean ± SD of triplicate experiments. For combination group compared to the single-agent group, unpaired *t*-test was used. $***p < 0.001$. CI was calculated using CalcuSyn.

assay. The result showed that the IC_{50} value ranged from 1 to 26 μM (Fig. 4c), implying a less pronounced inhibitory effect on tumor cell growth. Therefore, we wanted to verify whether the BCL-2 inhibitor APG-2575 combined with ibrutinib had a stronger antitumor proliferative effect in DLBCL. We observed that APG-2575 in combination with ibrutinib exhibited synergistic growth inhibition on BCL-2-overexpressing or BCL-2-intermediate and MCL-1-overexpressing cell lines OCI-LY8, OCI-LY1, and SU-DHL4, and the CI values of each cell line also

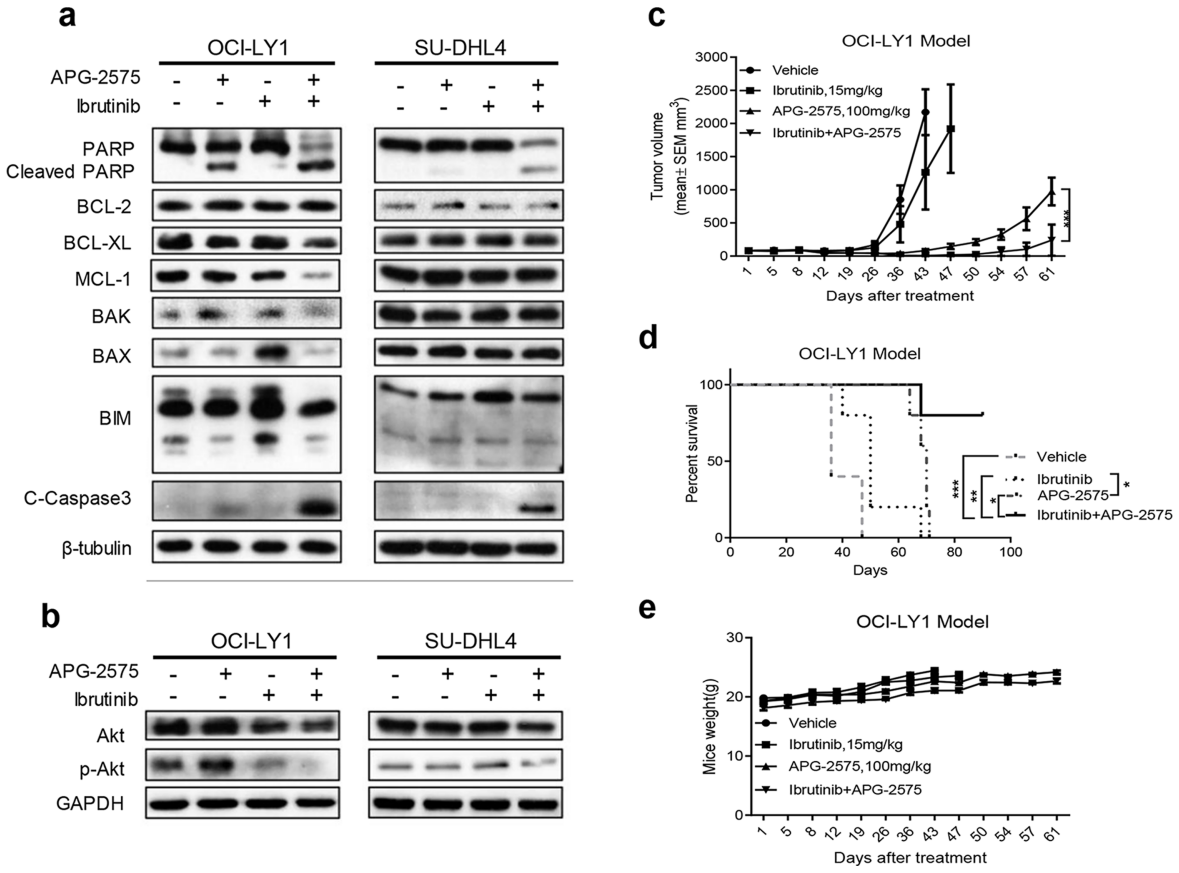

Figure 5. Combination of APG-2575 and ibrutinib induces decreased expression of MCL-1 and p-AKT. (a) OCI-LY1 and SU-DHL4 cells were treated with DMSO, APG-2575 (10 nM for OCI-LY1, 50 nM for SU-DHL4), ibrutinib (1 μM), or both agents for 24 h. Expression of BCL-2 family members and apoptosis proteins were determined by Western blot. β-Tubulin was used as a loading control. (b) Western blot was performed to detect the expression of Akt and p-Akt in OCI-LY1 and SU-DHL4 cells treated with DMSO, APG-2575 (10 nM for OCI-LY1, 50 nM for SU-DHL4), ibrutinib (1 μM), or both agents for 24 h. (c) Tumor growth of OCI-LY1 model treated with vehicle, APG-2575 (100 mg/kg), ibrutinib (15 mg/kg), and Combo. Data are shown as mean ± SEM of five mice in each group. Statistical significance was determined by two-way ANOVA. ***$p < 0.001$. (d) Kaplan–Meier survival curves of mice between the four groups. $n = 5$ per group; statistical significance was evaluated by the log rank test. **$p < 0.01$, *$p < 0.05$, ***$p < 0.001$. (e) Mice weight of the four separate groups was recorded. Data are shown as mean ± SD of five mice in each group of triplicate experiments.

showed synergistic effects (Fig. 4d–g). The combination of APG-2575 and ibrutinib significantly induced apoptosis compared with either drug alone, suggesting significant lethality of the combination (Fig. 4h–j).

We further explored the underlying mechanism of synergic effect between BCL-2 inhibition and BTK blockade. Western blot analysis revealed that ibrutinib treatment alone upregulated the expression of proapoptotic proteins Bax and Bim. Hence, combination of APG-2575 and ibrutinib could induce more obvious apoptosis with increasing expression of cleaved PARP and cleaved caspase 3 (Fig. 5a). Intriguingly, OCI-LY1 cells treated with APG-2575 could slightly upregulate the protein expression of MCL-1 and p-Akt, which could be reversed by ibrutinib treatment in the combination group (Fig. 5b). However, this phenomenon was not obvious in SU-DHL4 cells. In order to test the synergistic antitumor effect of cotreatment of APG-2575 and ibrutinib, the OCI-LY1 xenograft model was established. APG-2575 single agent could effectively delay tumor growth than vehicle and ibrutinib single agent. In addition, APG-2575 combined with ibrutinib significantly delayed tumor growth and prolonged mice survival than either agent alone (Fig. 5c and d). In addition, the mice body weight increased steadily even in the combination group of the two agents (Fig. 5e), which indicated the cotreatment of APG-2575 and ibrutinib was well tolerated. Altogether, these data demonstrated that BCL-2 inhibition combined with BTK blockade showed synergistic antitumor effect in DLBCL both in vitro and in vivo.

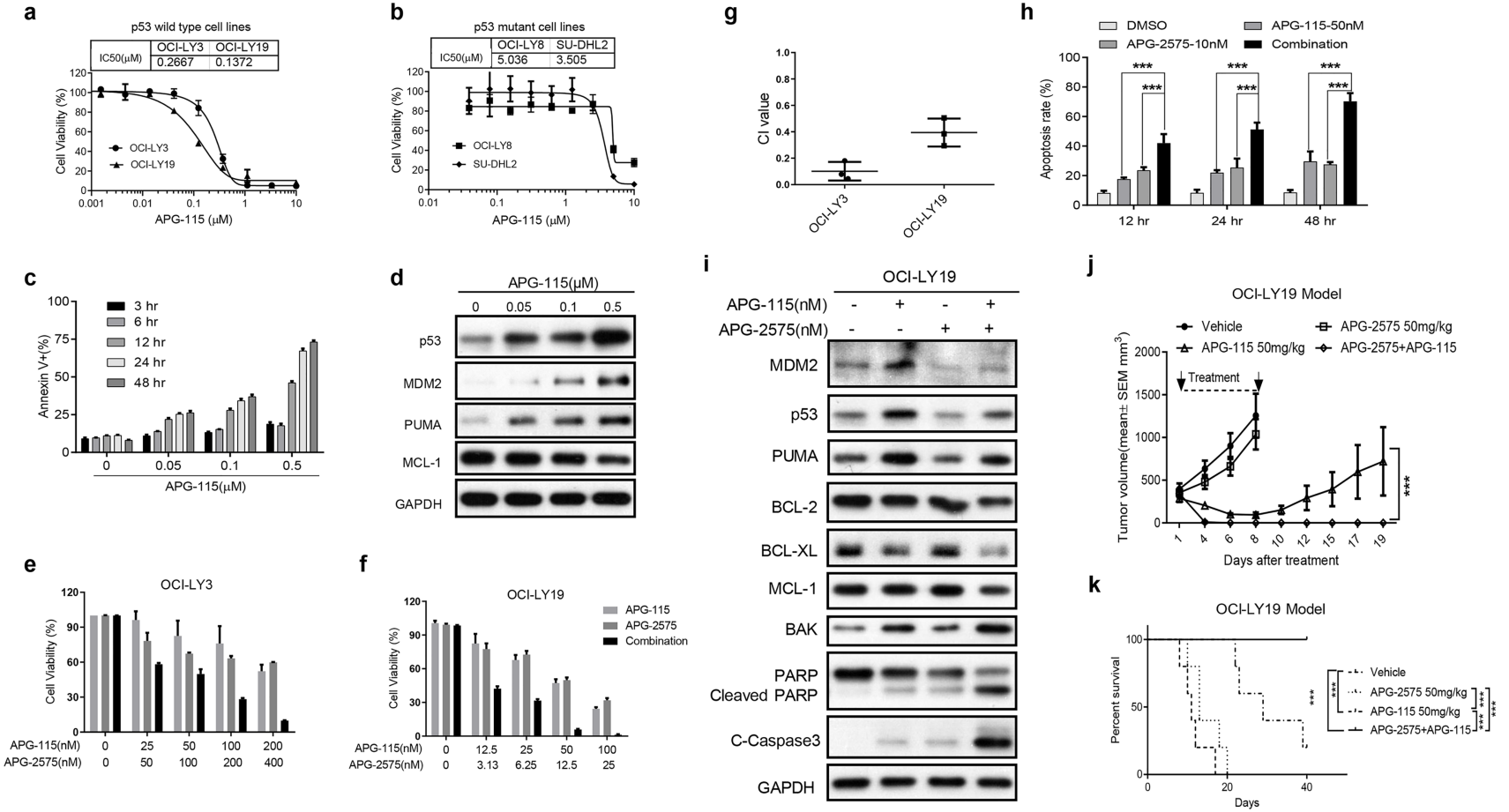

Figure 6. BCL-2 inhibition and p53 activation exhibit potent antitumor activity both in vitro and in vivo. (a) Cell viability of p53 wild-type DLBCL cell lines treated with APG-115 for 48 h, relative to cells treated with DMSO (100%). (b) Cell viability of p53 mutant type DLBCL cell lines treated with APG-115 for 48 h, relative to cells treated with DMSO (100%). The results in (a) and (b) represent the average and SD for three independent experiments. (c) OCI-LY19 cells treated with indicated dose of APG-115 at different time points, and then cells were harvested for apoptosis detection by flow cytometry. The data are presented as the mean ± SD of triplicate experiments. (d) Western blot analysis to evaluate the protein expression of p53, MDM2, PUMA, and MCL-1in OCI-LY19 cells treated with indicated concentrations of APG-115 for 24 h. GAPDH was used as the loading control. (e) Cell viability of OCI-LY3 cells after treatment with APG-115, APG-2575, or the combination at indicated concentrations for 48 h. (f) Cell viability of OCI-LY19 cells after treatment with APG-115, APG-2575, or the combination at indicated concentrations for 48 h. The data are presented as the mean ± SD of triplicate experiments. (g) CI value of the APG-2575 and APG-115 combination in OCI-LY3 and OCI-LY19 cells. CI value was calculated using CalcuSyn. (h) Apoptosis induction in OCI-LY19 cells after treatment with APG-115, APG-2575, or the combination at indicated time points. The data are presented as the mean ± SD of triplicate experiments. For combination group compared to single-agent group, unpaired *t*-test was used. ***$p < 0.001$. (i) OCI-LY19 cells were treated with DMSO, APG-115 (50 nM), APG-2575 (10 nM), or both agents for 24 h. Protein expression was determined by Western blot. GAPDH was used as a loading control. (j) Tumor growth of the OCI-LY19 model treated with vehicle, APG-2575 (50 mg/kg), APG-115 (50 mg/kg), and combination. Data represent the mean ± SEM of five mice examined in each group. Statistical significance was determined by two-way ANOVA. ***$p < 0.001$. (k) Kaplan–Meier survival curves of mice between the four groups. $n = 5$ per group; statistical significance was evaluated by the log rank test. ***$p < 0.001$.

BCL-2 Inhibition Combined With p53 Activation Exhibited Potent Antitumor Activity in p53 Wild-Type DLBCL With High Expression of BCL-2

The inactivation of p53 function is another important way for cancer cells to escape apoptosis. MDM2–p53 inhibitor can effectively relieve the inhibition of MDM2 on p53 and steadily restore the anticancer effect of p53. We first tested the antiproliferation of a novel MDM2–p53 inhibitor APG-115 in two p53 wild-type cells OCI-LY3 and OCI-LY19 as well as p53 mutant cells OCI-LY8 and SU-DHL2. We found that APG-115 could potently suppress cell proliferation in two p53 wild-type DLBCL cells but was less effective in p53 mutant cells (Fig. 6a and b), which demonstrated that APG-115 inhibited cell viability depending on wild-type p53. APG-115 could trigger a time- and dose-dependent cell apoptosis as well as p53 accumulation in OCI-LY19 (Fig. 6c). In addition, APG-115 could deregulate the expression of MCL-1, which is a key factor affecting the effectiveness of BCL-2 inhibitors (Fig. 6d).

Based on the above results, we considered to further explore whether the combination of BCL-2 inhibitor and activation of p53 pathway can achieve better antitumor effect in wild-type p53 DLBCL cells with BCL-2 overexpression. We treated two p53 wild-type OCI-LY3 and OCI-LY19 cells with increasing concentration of APG-2575 and APG-115 at a fixed proportion. We found that APG-2575 combined with APG-115 could synergistically reduce the cells' viability, and the mean CI values in OCI-LY3 and OCI-LY19 were 0.101 and 0.395, respectively (Fig. 6e–g). When used as a single agent at a lower concentration, APG-2575 and APG-115 could only produce weak apoptosis induction in OCI-LY19 cells. The combination of the two agents could induce more significant cell apoptosis in a time-dependent manner (Fig. 6h). Western blot analysis revealed that APG-115 alone could activate the p53–PUMA pathway, which is associated with apoptosis (Fig. 6i). APG-115 could synergize APG-2575 to upregulate the expression of BAK, cleaved PARP, and cleaved caspase 3 and decrease the expression of BCL-XL and MCL-1 (Fig. 6i). We further investigated the inhibitory effect of APG-2575 combined with APG-115 on OCI-LY19 transplanted tumor model of p53 wild-type cells. APG-115 alone significantly inhibited tumor growth, and tumor growth was rapidly increased after drug withdrawal (Fig. 6j). To our surprise, all the xenograft tumors in the combined group regressed after 6 days of treatment, and none recurred after 35 days of continuous observation (Fig. 6j). Compared with the vehicle and the APG-2575 group, APG-115 single agent significantly prolonged mice survival, and the combination therapy can cure the mice (Fig. 6k).

DISCUSSION

DLBCL is a molecularly heterogeneous disease in which approximately 20% of DLBCL patients have a translocation involving BCL-2/t (14;18). In our study, we first demonstrated a novel BCL-2 selective inhibitor, APG-2575, which was developed by Ascentage Pharma Group Inc (Taizhou, China), that exerted a potent antitumor effect in DLBCL.

We verified that in DLBCL cell lines, increased BCL-2 expression was associated with increased sensitivity to APG-2575, which was similar to that previously reported for BCL-2 inhibitors[9,31]. We found that APG-2575 induced cell apoptosis in a concentration- and time-dependent manner via upregulation of cleaved PARP and cleaved caspase 3. We also investigated the mechanism underlying the antitumor activity of APG-2575, and the result was consistent with a previous study[12]. Normally, pores in the mitochondrial membrane that caused MOMP and cytochrome c release into the cytosol are critical signal of caspase activation[32]. After treatment with APG-2575, the mitochondrial membrane potential changes and permeability increases, and cytochrome c is released into the cytosol, which rapidly triggers apoptosis. Since the release of cytochrome c is generally considered a feature of irreversible apoptosis, APG-2575 has a strong tumor-killing effect on sensitive DLBCL cell lines. These data suggest that APG-2575 induces apoptosis via activating the mitochondrial apoptotic pathway. In in vivo studies, we found that daily oral administration of APG-2575 inhibited the growth of OCI-LY8 subcutaneous xenografts in a dose-dependent manner. Even at 100 mg/kg, it was still well tolerated. APG-2575 effectively induced tumor cell apoptosis in vivo, which was consistent with in vitro studies. Therefore, BCL-2 inhibitor APG-2575 alone can effectively inhibit those DLCBL with high expression of BCL-2 and low expression of MCL-1.

It has been confirmed that BTK is one of the key molecules in the pathogenesis of B-cell malignancies including chronic lymphocytic leukemia (CLL) and ABC subtype of DLBCL, and many inhibitors for this target are developed[33]. However, BTK inhibitor ibrutinib has limited efficacy and can eventually cause drug resistance[16,21]. Combination therapy is one of the ways to overcome these obstacles[22]. A strong synergism between ibrutinib and BCL-2 inhibitor has been previously reported[33,34]. Similar results were observed in our study. We found that APG-2575 could significantly enhance the inhibitory effect of ibrutinib on DLBCL and increase apoptotic cell death, even in the GCB subtype DLBCL. In the OCI-LY1 cell transplantation model, APG-2575 can significantly sensitize the tumor growth suppression of ibrutinib. For the synergistic action of BCL-2 and BTK inhibitors, previous studies have proposed several possible mechanisms,

including increased BIM levels and decreased abundance or function of MCL-1[35,36]. In our study, the combination of APG-2575 and ibrutinib induced increasing expression of apoptotic proteins, including PARP and cleaved caspase 3. We also discovered the MCL-1 protein levels decreased in OCI-LY1 with the cotreatment of APG-2575 and ibrutinib. It has also been suggested that ibrutinib may inhibit MCL-1 function but not necessarily reduce its levels[37]. To our surprise, our study showed for the first time that combination therapy could reverse the increased p-Akt level caused by APG-2575 or ibrutinib in OCI-LY1 and SU-DHL4 cells, but the exact mechanism remains to be further explored. These data suggested that BCL-2 inhibition by APG-2575 can overcome the limitations of BTK inhibition and exert better antitumor effects.

TP53 is an important tumor suppressor gene, which is mutated in about 50% of human solid tumors, but rarely in hematologic malignancies[23]. The function of wild-type p53 is usually inhibited by MDM2, an E3 ubiquitin ligase targeting p53 for proteasome degradation[24]. The upregulation of antiapoptosis BCL-2 family members and inactivation of p53 function are two typical methods for tumor cells to escape apoptosis. It has been shown that high expression of MCL-1 is one of the reasons for poor efficacy of BCL-2 inhibitors, while p53 activation can negatively regulate the Ras/Raf/MEK/ERK pathway, activate GSK3 to regulate MCL-1 phosphorylation, and promote its degradation[28]. Therefore, we verified that the BCL-2 inhibitor APG-2575 in combination with the MDM2-P53 inhibitor APG-115 has a synergistic inhibitory effect and induced more significant apoptosis in the wild-type p53 DLBCL with BCL-2 overexpression and MCL-1 mean expression. APG-115 can induce cell cycle arrest and upregulate apoptosis-related protein PUMA by activating the function of p53, and APG-2575 can rapidly induce apoptosis in tumor cells through cell cycle arrest, achieving a synergistic effect. In addition, we also found that APG-115 combined with APG-2575 decreased the expression of antiapoptotic proteins BCL-2, BCL-XL, and MCL-1 and upregulated the expression of apoptotic effector BAK. In OCI-LY19 models, we saw a significant antitumor effect of the combination of APG-2575 and APG-115 on rapidity and radicality. Therefore, for those p53 wild-type DLBCL with BCL-2 overexpression and MCL-1 expression, the combination of BCL-2 inhibitor APG-2575 and MDM2-P53 inhibitor APG-115 resulted in a strong antitumor effect. However, the types of cell lines used in this study are limited and may require further validation in more DLBCL cell lines or even in patient-derived models.

Collectively, these data may provide preclinical evidence of an effective and precise therapeutic strategy for rational combination of APG-2575 and BTK inhibitor ibrutinib or MDM2-P53 inhibitor APG-115 in DLBCL, which warrants further clinical investigation.

ACKNOWLEDGMENTS: This study was supported by the National Natural Science Foundation of China (NSFC: 81101671, 81602066, and 81772587), the Natural Science Foundation of Guangdong Province (2016A030313280 and 2018A030310260), and The Medical Science Foundation of Guangdong Province (A2016023 and 2018102516469945). All data in our study are included in this published article, and the data in our study also have been recorded at Sun Yat-sen University Cancer Center for future reference (RDD number: RDDB2018000260). Conception and design of this study were carried out by M.Z.Q., D.J.Y., and J.S. Most of the experiments were conducted by Q.Y.L., W.T.P., and S.N.Z., including analyzing the data and writing the manuscript. X.L.Y., L.P.Y., and G.F.W. preformed the animal experiments. L.Z. and H.J.Y. provided support for the animal experiments. Z.Y.L., J.W., and H.B.C. conducted apoptosis-associated assays and Western blot analysis. M.X.P. and Y.X.Z. helped analyze the experiment data and edit the manuscript. Da-Jun Yang has ownership interest (including patents) in Ascentage Pharma Group Corp. Limited. Wentao Pan and Guangfeng Wang are employees of Ascentage Pharma Group Corp. Limited. The authors declare no conflicts of interest.

REFERENCES

1. Shankland KR, Armitage JO, Hancock BW. Non-Hodgkin lymphoma. Lancet 2012;380(9844):848–57.
2. Siegel RL, Miller KD, Jemal A. Cancer statistics, 2018. CA Cancer J Clin. 2018;68(1):7–30.
3. Kubuschok B, Held G, Pfreundschuh M. Management of diffuse large B-cell lymphoma (DLBCL). Cancer Treat Res. 2015;165:271–88.
4. Li S, Young KH, Medeiros LJ. Diffuse large B-cell lymphoma. Pathology 2018;50(1):74–87.
5. Iqbal J, Neppalli VT, Wright G, Dave BJ, Horsman DE, Rosenwald A, Lynch J, Hans CP, Weisenburger DD, Greiner TC, Gascoyne RD, Campo E, Ott G, Müller-Hermelink HK, Delabie J, Jaffe ES, Grogan TM, Connors JM, Vose JM, Armitage JO, Staudt LM, Chan WC. BCL2 expression is a prognostic marker for the activated B-cell-like type of diffuse large B-cell lymphoma. J Clin Oncol. 2006;24(6):961–8.
6. Strasser A, Cory S, Adams JM. Deciphering the rules of programmed cell death to improve therapy of cancer and other diseases. EMBO J. 2011;30(18):3667–83.
7. Ng SY, Davids MS. Selective Bcl-2 inhibition to treat chronic lymphocytic leukemia and non-Hodgkin lymphoma. Clin Adv Hematol Oncol. 2014;12(4):224–9.
8. Sawas A, Diefenbach C, O'Connor OA. New therapeutic targets and drugs in non-Hodgkin's lymphoma. Curr Opin Hematol. 2011;18(4):280–7.
9. Tse C, Shoemaker AR, Adickes J, Anderson MG, Chen J, Jin S, Johnson EF, Marsh KC, Mitten MJ, Nimmer P, Roberts L, Tahir SK, Xiao Y, Yang X, Zhang H, Fesik S, Rosenberg SH, Elmore SW. ABT-263: A potent and orally bioavailable Bcl-2 family inhibitor. Cancer Res. 2008;68(9):3421–8.
10. Oltersdorf T, Elmore SW, Shoemaker AR, Armstrong RC, Augeri DJ, Belli BA, Bruncko M, Deckwerth TL, Dinges J, Hajduk PJ, Joseph MK, Kitada S, Korsmeyer SJ, Kunzer AR, Letai A, Li C, Mitten MJ, Nettesheim DG, Ng S, Nimmer PM, O'Connor JM, Oleksijew A, Petros AM, Reed JC, Shen W, Tahir SK, Thompson CB, Tomaselli KJ,

Wang B, Wendt MD, Zhang H, Fesik SW, Rosenberg SH. An inhibitor of Bcl-2 family proteins induces regression of solid tumours. Nature 2005;435(7042):677–81.
11. Timucin AC, Basaga H, Kutuk O. Selective targeting of antiapoptotic BCL-2 proteins in cancer. Med Res Rev. 2019;39(1):146–75.
12. Souers AJ, Leverson JD, Boghaert ER, Ackler SL, Catron ND, Chen J, Dayton BD, Ding H, Enschede SH, Fairbrother WJ, Huang DC, Hymowitz SG, Jin S, Khaw SL, Kovar PJ, Lam LT, Lee J, Maecker HL, Marsh KC, Mason KD, Mitten MJ, Nimmer PM, Oleksijew A, Park CH, Park CM, Phillips DC, Roberts AW, Sampath D, Seymour JF, Smith ML, Sullivan GM, Tahir SK, Tse C, Wendt MD, Xiao Y, Xue JC, Zhang H, Humerickhouse RA, Rosenberg SH, Elmore SW. ABT-199, a potent and selective BCL-2 inhibitor, achieves antitumor activity while sparing platelets. Nat Med. 2013;19(2):202–8.
13. Gandhi L, Camidge DR, de Oliveira MR, Bonomi P, Gandara D, Khaira D, Hann CL, McKeegan EM, Litvinovich E, Hemken PM, Dive C, Enschede SH, Nolan C, Chiu YL, Busman T, Xiong H, Krivoshik AP, Humerickhouse R, Shapiro GI, Rudin CM. Phase I study of navitoclax (ABT-263), a novel Bcl-2 family inhibitor, in patients with small-cell lung cancer and other solid tumors. J Clin Oncol. 2011;29(7):909–16.
14. Rudin CM, Hann CL, Garon EB, de Oliveira MR, Bonomi PD, Camidge DR, Chu Q, Giaccone G, Khaira D, Ramalingam SS, Ranson MR, Dive C, McKeegan EM, Chyla BJ, Dowell BL, Chakravartty A, Nolan CE, Rudersdorf N, Busman TA, Mabry MH, Krivoshik AP, Humerickhouse RA, Shapiro GI, Gandhi. Phase II study of single-agent navitoclax (ABT-263) and biomarker correlates in patients with relapsed small cell lung cancer. Clin Cancer Res. 2012;18(11):3163–9.
15. Das M. Venetoclax active and safe in non-Hodgkin lymphoma. Lancet Oncol. 2017;18(3):e136.
16. Blum KA. B-cell receptor pathway modulators in NHL. Hematology Am Soc Hematol Educ Program 2015;2015: 82–91.
17. Niemann CU, Wiestner A. B-cell receptor signaling as a driver of lymphoma development and evolution. Semin Cancer Biol. 2013;23(6):410–21.
18. Davis RE, Ngo VN, Lenz G, Tolar P, Young RM, Romesser PB, Kohlhammer H, Lamy L, Zhao H, Yang Y, Xu W, Shaffer AL, Wright G, Xiao W, Powell J, Jiang JK, Thomas CJ, Rosenwald A, Ott G, Muller-Hermelink HK, Gascoyne RD, Connors JM, Johnson NA, Rimsza LM, Campo E, Jaffe ES, Wilson WH, Delabie J, Smeland EB, Fisher RI, Braziel RM, Tubbs RR, Cook JR, Weisenburger DD, Chan WC, Pierce SK, Staudt LM. Chronic active B-cell-receptor signalling in diffuse large B-cell lymphoma. Nature 2010;463(7277):88–92.
19. Alinari L, Quinion C, Blum KA. Bruton's tyrosine kinase inhibitors in B-cell non-Hodgkin's lymphomas. Clin Pharmacol Ther. 2015;97(5):469–77.
20. Valla K, Flowers CR, Koff JL. Targeting the B cell receptor pathway in non-Hodgkin lymphoma. Expert Opin Investig Drugs 2018;27(6):513–22.
21. Wilson WH, Young RM, Schmitz R, Yang YD, Pittaluga S, Wright G, Lih CJ, Williams PM, Shaffer AL, Gerecitano J, de Vos S, Goy A, Kenkre VP, Barr PM, Blum KA, Shustov A, Advani R, Fowler NH, Vose JM, Elstrom RL, Habermann TM, Barrientos JC, McGreivy J, Fardis M, Chang BY, Clow F, Munneke B, Moussa D, Beaupre DM, Staudt LM. Targeting B cell receptor signaling with ibrutinib in diffuse large B cell lymphoma. Nat Med. 2015;21(8):922–6.
22. Zhang SQ, Smith SM, Zhang SY, Lynn Wang Y. Mechanisms of ibrutinib resistance in chronic lymphocytic leukaemia and non-Hodgkin lymphoma. Br J Haematol. 2015; 170(4):445–56.
23. Cerami E, Gao J, Dogrusoz U, Gross BE, Sumer SO, Aksoy BA, Jacobsen A, Byrne CJ, Heuer ML, Larsson E, Antipin Y, Reva B, Goldberg AP, Sander C, Schultz N. The cBio cancer genomics portal: An open platform for exploring multidimensional cancer genomics data. Cancer Discov. 2012;2(5):401–4.
24. Kruiswijk F, Labuschagne CF, Vousden KH. p53 in survival, death and metabolic health: A lifeguard with a licence to kill. Nat Rev Mol Cell Biol. 2015;16(7):393–405.
25. Qin JJ, Li X, Hunt C, Wang W, Wang H, Zhang R. Natural products targeting the p53-MDM2 pathway and mutant p53: Recent advances and implications in cancer medicine. Genes Dis. 2018;5(3):204–19.
26. Konopleva M, Contractor R, Tsao T, Samudio I, Ruvolo PP, Kitada S, Deng X, Zhai D, Shi YX, Sneed T, Verhaegen M, Soengas M, Ruvolo VR, McQueen T, Schober WD, Watt JC, Jiffar T, Ling X, Marini FC, Harris D, Dietrich M, Estrov Z, McCubrey J, May WS, Reed JC, Andreeff M. Mechanisms of apoptosis sensitivity and resistance to the BH3 mimetic ABT-737 in acute myeloid leukemia. Cancer Cell 2006;10(5):375–88.
27. Chen S, Dai Y, Harada H, Dent P, Grant S. Mcl-1 down-regulation potentiates ABT-737 lethality by cooperatively inducing Bak activation and Bax translocation. Cancer Res. 2007;67(2):782–91.
28. Pan R, Ruvolo V, Mu H, Leverson JD, Nichols G, Reed JC, Konopleva M, Andreeff M. Synthetic lethality of combined Bcl-2 inhibition and p53 activation in AML: Mechanisms and superior antileukemic efficacy. Cancer Cell 2017;32(6):748–60.e6.
29. Yi H, Yan X, Luo Q, Yuan L, Li B, Pan W, Zhang L, Chen H, Wang J, Zhang Y, Zhai Y, Qiu MZ, Yang DJ. A novel small molecule inhibitor of MDM2-p53 (APG-115) enhances radiosensitivity of gastric adenocarcinoma. J Exp Clin Cancer Res. 2018;37(1):97.
30. Carreon-Burciaga RG, Gonzalez-Gonzalez R, Molina-Frechero N, Bologna-Molina R. Immunoexpression of Ki-67, MCM2, and MCM3 in ameloblastoma and ameloblastic carcinoma and their correlations with clinical and histopathological patterns. Dis Markers 2015;2015:683087.
31. Peirs S, Matthijssens F, Goossens S, Van de Walle I, Ruggero K, de Bock CE, Degryse S, Cante-Barrett K, Briot D, Clappier E, Lammens T, De Moerloose B, Benoit Y, Poppe B, Meijerink JP, Cools J, Soulier J, Rabbitts TH, Taghon T, Speleman F, Van Vlierberghe P. ABT-199 mediated inhibition of BCL-2 as a novel therapeutic strategy in T-cell acute lymphoblastic leukemia. Blood 2014;124(25):3738–47.
32. Kuwana T, Mackey MR, Perkins G, Ellisman MH, Latterich M, Schneiter R, Green DR, Newmeyer DD. Bid, Bax, and lipids cooperate to form supramolecular openings in the outer mitochondrial membrane. Cell 2002;111(3):331–42.
33. Wang Y, Zhang LL, Champlin RE, Wang ML. Targeting Bruton's tyrosine kinase with ibrutinib in B-cell malignancies. Clin Pharmacol Ther. 2015;97(5):455–68.
34. Kuo HP, Ezell SA, Schweighofer KJ, Cheung LWK, Hsieh S, Apatira M, Sirisawad M, Eckert K, Hsu SJ, Chen CT, Beaupre DM, Versele M, Chang BY. Combination of ibrutinib and ABT-199 in diffuse large B-cell lymphoma

and follicular lymphoma. Mol Cancer Ther. 2017;16(7): 1246–56.
35. Moore VD, Brown JR, Certo M, Love TM, Novina CD, Letai A. Chronic lymphocytic leukemia requires BCL2 to sequester prodeath BIM, explaining sensitivity to BCL2 antagonist ABT-737. J Clin Invest. 2007;117(1):112–21.
36. Cervantes-Gomez F, Lamothe B, Woyach JA, Wierda WG, Keating MJ, Balakrishnan K, Gandhi V. Pharmacological and protein profiling suggests venetoclax (ABT-199) as optimal partner with ibrutinib in chronic lymphocytic leukemia. Clin Cancer Res. 2015;21(16):3705–15.
37. Deng J, Isik E, Fernandes SM, Brown JR, Letai A, Davids MS. Bruton's tyrosine kinase inhibition increases BCL-2 dependence and enhances sensitivity to venetoclax in chronic lymphocytic leukemia. Leukemia 2017;31(10): 2075–84.